The Nonunitarity of Finite-Element Beam Propagation Algorithms

Henghua Deng and David Yevick, *Fellow, IEEE*

***Abstract*—We examine the intrinsic nonunitarity of one-way finite-element propagation techniques in order to clarify the results of previous authors.**

***Index Terms*—Electric field propagation, integrated optics, numerical techniques.**

I. Introduction

WHILE numerous numerical simulations of optical devices have been performed with explicitly stable one-way scalar finite-difference electrical field propagation methods, electric field polarization evolution in complex waveguiding geometries is often better described by vectorial finite-element procedures. However, as discussed below, these intrinsically violate power-conservation. While this effect can be reduced by, e.g., absorbing propagators or boundary conditions (BCs), power losses still cannot be reliably estimated.

II. Propagation Methods

The scalar Helmholtz equation for the spatial component of a monochromatic transverse-electric (TE) polarized field [1], [2]

$$\left(\frac{\partial^2}{\partial x^2}+\frac{\partial^2}{\partial y^2}+\frac{\partial^2}{\partial z^2}+k_0^2n^2\right)\mathbf{E}=0 \tag{1}$$

can be transformed into power-conserving one-way propagation procedures [1]–[3] although the field power is normally identified with, e.g., the L_2 norm in the paraxial approximation, rather than the Poynting vector [4]–[7]. On the other hand, the corresponding approach for transverse-magnetic (TM) waves generally violates power conservation when the derivative of the refractive index in the propagation direction is neglected [8] although methods have recently been found to include this term [9]–[11].

A full vectorial one-way description of the modes of a guided electromagnetic field is given by the magnetic field eigenvalue equation [12], [13]

$$\nabla_t^2\mathbf{H}_t+k_0^2n^2\mathbf{H}_t+\frac{1}{n^2}[\nabla_t n^2\times(\nabla_t\times\mathbf{H}_t)]=\beta^2\mathbf{H}_t \tag{2}$$

or the equivalent electric field formalism [5], [12]. However, the third operator in the left-hand side of (2) is not self-adjoint (therefore, neither symmetric nor Hermitian) in Hilbert space (cf. [5], [14] and [12, Th. 1]), and may contribute to the occurrence of complex modes [12], [15] in vectorial algorithms. This problem is especially severe at discrete index steps where field patterns may in certain circumstances become singular [11], [8]. As a result, in finite-difference algorithms directly solving the differential form (2), matrices are non-Hermitian once the third operator is included [13]. However, in finite-element schemes with appropriate variational techniques [14], from the functional of (2), we can obtain the generalized eigenvalue equation

$$[K]\{\Phi\}-\beta^2[M]\{\Phi\}=\{0\} \tag{3}$$

with Hermitian (real and symmetric) and sparse matrices $[K]$ and $[M]$ for lossless isotropic dielectrics subject to Dirichlet or Neumann BC. Here $\{0\},\beta$ and $\{\Phi\}$ represent the null vector, propagation constant, and $\mathbf{E}$ or $\mathbf{H}$ in the electric or magnetic field formalisms, respectively. For the mixed element procedure employed in this text, $[K]$ and $[M]$ can be constructed according to either [16]–[18] or [19].

Turning to propagation, in the slowing varying envelope approximation, after writing $\Phi=\phi e^{-jk_0n_0z}$ and neglecting derivatives with respect to z past a certain order we obtain

$$-2jk_0n_0[\tilde{M}]\frac{d\{\phi\}}{dz}+\left([K]-k_0^2n_0^2[M]\right)\{\phi\}=\{0\} \tag{4}$$

where $[\tilde{M}]=[M]+(1/(4k_0^2n_0^2))([K]-k_0^2n_0^2[M])$ and $[\check{M}]=[M]$ correspond to the wide-angle and paraxial approximations, respectively. The reference refractive index n_0 can be recomputed for each step for enhanced numerical accuracy [6], [20], [17]. Applying the Crank–Nicholson procedure to (4) yields

$$[A]\{\phi\}|_{z+\triangle z}=[B]\{\phi\}|_z \tag{5}$$

where [17]

$$[A]=-2jk_0n_0[\tilde{M}]+0.5\triangle z\left([K]-k_0^2n_0^2[M]\right) \tag{6}$$

$$[B]=-2jk_0n_0[\tilde{M}]-0.5\triangle z\left([K]-k_0^2n_0^2[M]\right). \tag{7}$$

We evaluate the optical power as in [18].

Although any expression of the form $(1-cjH)^{-1}(1+cjH)$ is unitary if H is Hermitian, this is not the case for the propagation operator associated with (5), which can clearly be written as

$$\{\phi\}|_{z+\triangle z}=(1-j[Q]\triangle z)^{-1}(1+j[Q]\triangle z)\{\phi\}|_z \tag{8}$$

Manuscript received October 22, 2004; revised February 9, 2005. This work was supported by the Canadian Institute for Photonic Innovations (CIPI), and by the Natural Science and Engineering Research Council of Canada (NSERC).

H. Deng is with the Department of Electrical and Computer Engineering, University of Waterloo, Waterloo, ON N2L 3G1, Canada (e-mail: hdeng@uwaterloo.ca).

D. Yevick is with the Department of Physics, University of Waterloo, Waterloo, ON N2L 3G1, Canada (e-mail: yevick@uwaterloo.ca).

Digital Object Identifier 10.1109/LPT.2005.848328

1041-1135/$20.00 © 2005 IEEE

where $[Q] = (1/(4k_0n_0))[\tilde{M}]^{-1}([K] - k_0^2n_0^2[M])$. However, even if $[K]$ and $[\tilde{M}]$ are Hermitian, so that $[\tilde{M}]^{-1}$ is Hermitian, the product $[\tilde{M}]^{-1}[K]$ is not Hermitian unless the two matrices commute (since $(PQ)^\dagger = Q^\dagger P^\dagger$) (this point was seemingly misunderstood in [19]). Therefore, complex modes may be present even if both matrices in (3) are Hermitian [15], [14], resulting in divergences of the associated propagation algorithms [1], [8]. These complex modes appear when neither $[K]$ nor $[M]$ are positive- or negative-definite [15], which is the case for the mixed element procedure [16]–[18] as $\det([K]) = \det([M]) = 0$. By introducing artificial dissipation into the Crank–Nicholson procedure [13] or applying highly absorbing BCs [21], the divergence can generally be suppressed but physical losses then cannot be reliably estimated. Complex Padé approximations [21], or nonphysical dissipative operators [7] are better techniques for ensuring stability but still possess the same intrinsic difficulty.

While at least one vectorial mixed element finite-element beam propagation method (FE-BPM) has been reported to be fully energy-conserving [19], it should be noted that in the presence of complex-conjugate eigenmode pairs, the Poynting vector of the field can be preserved [15], [12] at the same time that one of the magnetic and electric fields approaches infinity while the other field approaches zero. In this case, the field distributions generally become dominated by high-frequency modal components [21], [22], [8], [9], [10]. Additionally, after the transformation $\phi_z = j(\partial/\partial z)\phi'_z$ in [19], although the Poynting vector of the modified field $\{\phi_t, \phi'_z\}$ is preserved, this may not be the case for the physical field $\{\phi_t, \phi_z\}$.

III. Results

We now illustrate the above considerations by examining the numerical instabilities associated with a finite-element analysis of the high-index-contrast asymmetric silicon-on-insulator slanted-facet rib waveguide [23] of Fig. 1. The waveguide parameters are: facet angle $\theta = 54.736°$, rib height $H = 3\ \mu$m, rib base width $W = 3.3\ \mu$m, and outer-slab thickness $h = 1.1\ \mu$m. The refractive index of the silicon guiding and substrate layers is $n_1 = 3.48$, and that of the SiO_2 insulator is $n_2 = 1.45$. This device acts as a single section monomode (two orthogonal polarizations) polarization rotator (PR) with an optical axis positioned at 45° to the horizontal TE polarization direction, as described in our previous paper [23]. That is, after a half-beat length, the output is TM polarized for a TE input field [23].

We apply the Dirichlet BC in the full-vectorial mixed-element **H**-formulation FEM eigenmode solver of [16] together with the BPM procedure of [17]. Our calculations are performed on both the uniform mesh of Fig. 1(a) and the adaptive mesh of Fig. 1(b).

In Fig. 2, we display the eigenmode spectrum of the slanted angle waveguide for the regular mesh. The propagation constant of the lowest order fundamental eigenmode was also verified by the Crank–Nicholson imaginary distance BPM [9] with a propagation step-size $\triangle z = 0.1\ \mu$m, establishing the consistency of the propagation and eigenvalue methods. The numerous complex-conjugate eigenmode pairs lead as expected to divergences during field propagation as evident from Fig. 3, which shows the power in the propagating field normalized to the input

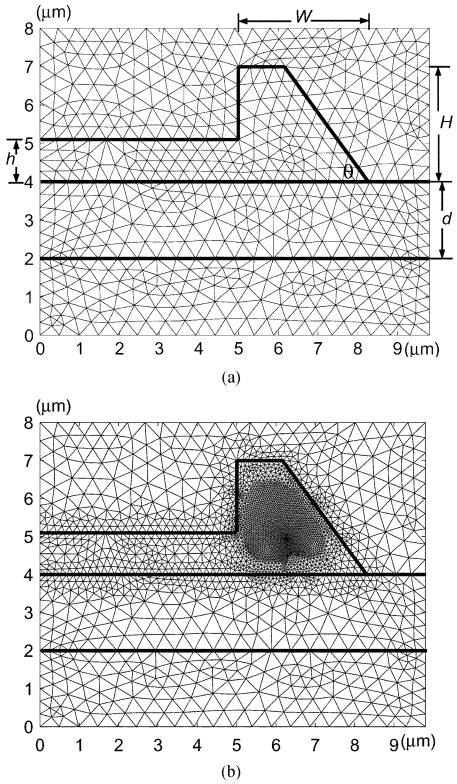


Fig. 1. Geometry and discretization of the waveguide cross section. Finite-element discretizations for the slanted-angle rib waveguide discussed in the text for (a) a regular mesh with 1156 elements, 622 nodes and minimum triangle area $1.47 \times 10^{-2}\ \mu$m^2; (b) an adaptive mesh with 6413 triangles, 3253 points and minimum triangle area $2.40 \times 10^{-4}\ \mu$m^2.

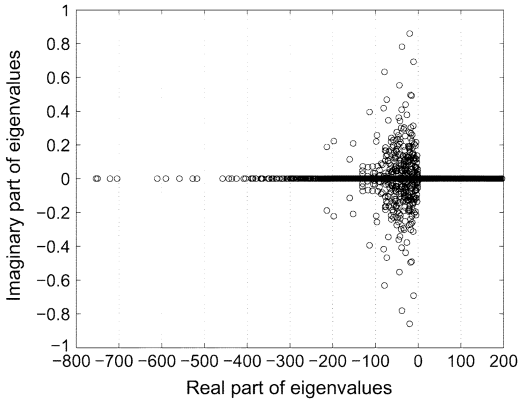


Fig. 2. Eigenmode spectrum for the mesh of Fig. 1(a).

power. Diverging oscillations in the power are first apparent at a 250-μm propagation distance for the uniform mesh while a corresponding instability (not shown) appears at 33 μm for the adaptive mesh due to the smaller grid point spacing for elements near index discontinuities.

Despite the instability at longer propagation lengths, the propagation method can still be employed to solve practical modeling problems. For example, the adaptive z-dependent complex reference index technique of [20] yields the normalized power for a TE-input field shown in Fig. 4. While this result is affected by the field divergence, similar calculations for low index contrast InGaAsP slanted-angle PR [23] remain stable. Further, the

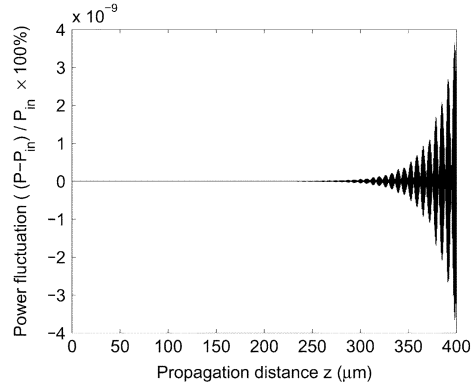


Fig. 3. Power fluctuation for the lowest-order fundamental mode as a function of propagation distance for the mesh of Fig. 1(a).

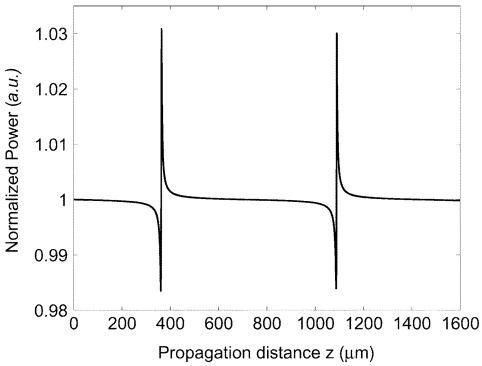


Fig. 4. Power versus propagation distance for the slanted angle waveguide excited by its TE polarized mode with the mesh of Fig. 1(a).

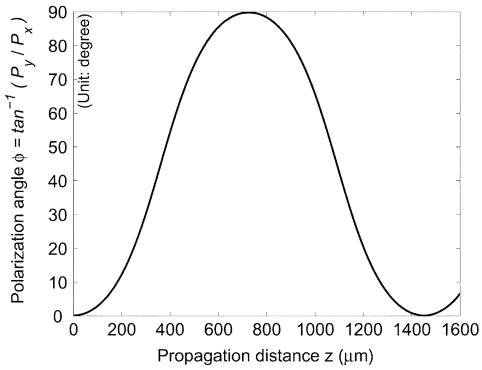


Fig. 5. Power transfer between the two guided modes of the slanted angle waveguide excited by its TE polarized mode as a function of propagation distance based on the mesh of Fig. 1(a).

power transfer between the TE and TM modes is correctly predicted, as evidenced from Fig. 5 which displays the polarization angle, $\phi = \tan^{-1}(P_y/P_x)$, obtained from the ratio of the power in the two polarization components.

IV. Conclusion

While mixed finite-element propagation procedures generally do not conserve power, practical calculations can still be performed for many waveguide profiles. Large discontinuous refractive index steps or small numerical grid spacings, however, result in rapid field divergences. Unfortunately, our results indicate that such divergences can easily occur for adaptive grids, for which the grid sizes near discontinuities typically become uncharacteristically small. While a solution similar to that of [3] and [22] may exist, the required analysis would be complex and therefore beyond the scope of this letter.

References

[1] D. Yevick, "A guide to electric field propagation techniques for guided-wave optics (invited paper)," *Opt. Quantum Electron.*, vol. 26, pp. S185–S197, 1994.

[2] D. Schulz, C. Glingener, and E. Voges, "Novel generalized finite-difference beam propagation method," *IEEE J. Quantum Electron.*, vol. 30, no. 4, pp. 1132–1140, Apr. 1994.

[3] B. Hermansson, D. Yevick, W. Bardyszewski, and M. Glasner, "The unitarity of split-operator finite difference and finite-element methods: Applications to longitudinally varying semiconductor rib waveguides," *J. Lightw. Technol.*, vol. 8, no. 12, pp. 1866–1873, Dec. 1990.

[4] J. Haes *et al.*, "A comparison between different propagative schemes for the simulation of tapered step index slab waveguides," *J. Lightw. Technol.*, vol. 14, no. 6, pp. 1557–1569, Jun. 1996.

[5] H. J. W. M. Hoekstra, "On beam propagation methods for modeling in integrated optics," *Opt. Quantum Electron.*, vol. 29, pp. 157–171, 1997.

[6] F. Schmidt, "An adaptive approach to the numerical solution of Fresnel's wave equation," *J. Lightw. Technol.*, vol. 11, no. 9, pp. 1425–1434, Sep. 1993.

[7] C. Vassallo, "Wide-angle BPM and power conservation," *Electron. Lett.*, vol. 31, no. 2, pp. 130–131, Jan. 1995.

[8] ——, "Difficulty with vectorial BPM," *Electron. Lett.*, vol. 33, no. 1, pp. 61–62, Jan. 1997.

[9] D. Yevick and B. Hermansson, "New approach to lossy optical waveguide," *Electron. Lett.*, vol. 21, pp. 1029–1030, Oct. 1985.

[10] J. Yamauchi, K. Matsubara, T. Tsuda, and H. Nakano, "Norm-conserving finite-difference beam-propagation method for TM wave analysis in step-index optical waveguides," *J. Lightw. Technol.*, vol. 18, no. 5, pp. 721–727, May 2000.

[11] L. Poladian and F. Ladouceur, "Unification of TE and TM beam-propagation algorithms," *IEEE Photon. Technol. Lett.*, vol. 10, no. 1, pp. 105–107, Jan. 1998.

[12] T. F. Jabłoñski, "Complex modes in open lossless dielectric waveguides," *J. Opt. Soc. Amer. A*, vol. 11, no. 4, pp. 1272–1282, Apr. 1994.

[13] C. L. Xu and W. P. Huang, "Finite-difference beam-propagation method for guide-wave optics," in *Progress in Electromagnetic Waves: PIERS 11*, W. P. Huang, Ed. Cambridge, MA: EMW Publishing, 1995, pp. 1–49.

[14] Y. Lu and F. A. Fernández, "An efficient finite element solution of inhomogeneous anisotropic & lossy dielectric waveguides," *IEEE Trans. Microw. Theory Tech.*, vol. 41, no. 6, pp. 1215–1223, Jun. 1993.

[15] M. Mrozowski, *Guided Electromagnetic Waves: Properties and Analysis*, U.K.: Research Studies Press Ltd./Wiley, 1997.

[16] M. Koshiba and Y. Tsuji, "Curvilinear hybrid edge/nodal elements with triangular shape for guided-wave problems," *J. Lightw. Technol.*, vol. 18, no. 5, pp. 737–743, May 2000.

[17] Y. Tsuji and M. Koshiba, "Adaptive mesh generation for full-vectorial guided-mode and beam-propagation solutions," *IEEE J. Sel. Topics Quantum Electron.*, vol. 6, no. 1, pp. 163–169, Jan./Feb. 2000.

[18] T. Fujisawa and M. Koshiba, "Finite element characterization of chromatic dispersion in nonlinear holey fibers," *OSA Opt. Express*, vol. 11, no. 13, pp. 1481–1489, Jun. 2003.

[19] D. Schulz, C. Glingener, M. Bludszuweit, and E. Voges, "Mixed finite element beam propagation method," *J. Lightw. Technol.*, vol. 16, no. 7, pp. 1336–1342, Jul. 1998.

[20] F. Schmidt and R. März, "On the reference wave vector of paraxial Helmholtz equations," *J. Lightw. Technol.*, vol. 14, no. 10, pp. 2395–2400, Oct. 1996.

[21] D. Yevick, "The application of complex Páde approximants to vector field propagation," *IEEE Photon. Technol. Lett.*, vol. 12, no. 12, pp. 1636–1638, Dec. 2000.

[22] D. Yevick, J. Yu, W. Bardyszewski, and M. Glasner, "Stability issues in vector electric field propagation," *IEEE Photon. Technol. Lett.*, vol. 7, no. 6, pp. 658–660, Jun. 1995.

[23] H. Deng, D. O. Yevick, C. Brooks, and P. E. Jessop, "Design rules for slanted-angle polarization rotators," *J. Lightw. Technol.*, vol. 23, no. 1, pp. 432–445, Jan. 2005.